Curious variant of the Bronnikov-Ellis spacetime

Sayan Kar*
Department of Physics, Indian Institute of Technology Kharagpur, Kharagpur 721 302, India

(Received 17 August 2021; accepted 7 December 2021; published 4 January 2022; corrected 17 March 2022)

We explore a curious but simple variant of the Bronnikov-Ellis wormhole spacetime with a specific "redshift function" (i.e. g_{00}) in the line element. The matter required to support such a geometry violates the local null energy condition (NEC) only around the throat and the global averaged NEC integral along radial null geodesics may be adjusted to arbitrarily small negative values, using metric parameters. Properties of the line element manifest in the metric functions, curvature and the required matter stress energy are delineated. Further, exact null and timelike geodesics are found and generic features of periodic/nonperiodic motion (closed, bounded or open) are presented. Scalar wave propagation is also solved analytically, thereby providing a partial check on the stability of the geometry under scalar perturbations. Interestingly, we note that this Bronnikov-Ellis variant may be viewed as a four dimensional, timelike section of a five dimensional, static, nonvacuum, Witten bubblelike geometry which, with an extra dimension, also has wormhole features and is threaded by matter satisfying the NEC.

DOI: 10.1103/PhysRevD.105.024013

I. INTRODUCTION

The Bronnikov-Ellis (BE) spacetime [1,2] has been studied extensively over many years, by numerous authors. It is known as an example of a Lorentzian wormhole geometry. Even though the matter stress energy required to support this geometry consists of an energy-condition violating, negative kinetic energy scalar field, the simplicity of the line element (at least in a special case) is perhaps a reason behind its popularity. It is also true that not many "exact solutions" are known for Lorentzian wormholes and BE presents a useful example.

Let us first recall the line element. It is given as

$$ds^2 = -e^{f(l)}dt^2 + e^{-f(l)}[dl^2 + (b_0^2 + l^2)d\Omega_2^2], \quad (1)$$

where $f(l) = \frac{M}{b_0}(\arctan\frac{l}{b_0} - \frac{\pi}{2})$.

The phantom (negative kinetic energy) scalar field configuration $\phi(l)$ is

$$\phi(l) = \frac{D}{b_0}\left(\arctan\frac{l}{b_0} - \frac{\pi}{2}\right), \quad (2)$$

where we have $4D^2 = M^2 + 4b_0^2$.

A simple special case arises for $M = 0$, for which we have $D = b_0$ and the line element becomes

$$ds^2 = -dt^2 + dl^2 + (b_0^2 + l^2)d\Omega_2^2. \quad (3)$$

Using the standard "r" coordinate, we can rewrite the above line element as

$$ds^2 = -dt^2 + \frac{dr^2}{1 - \frac{b_0^2}{r^2}} + r^2 d\Omega_2^2. \quad (4)$$

The $t =$ constant, $\theta = \frac{\pi}{2}$ sections of the $M = 0$ BE spacetime are catenoids—two-dimensional spaces with zero mean curvature. Numerous investigations on various aspects of this special case have been carried out in the past [3–6] and also recently [7–19]. It has been suggested that Lorentzian wormholes in general and BE geometry (including its variants) in particular, could be useful examples of black hole mimickers in the context of gravitational wave physics [20–26].

The original BE spacetime, as evident from (1), does have a nontrivial "redshift function" (i.e. $g_{00} = -e^{f(l)}$). Here we consider a different "redshift function" which ensures a local violation (around the wormhole throat) of only one of the null energy condition (NEC) inequalities. We shall see that the averaged null energy condition (ANEC) violation may also be controlled by choosing appropriate values of the metric parameters (e.g. macroscopic wormholes with large throat radii). Further, as we show and discuss below, our geometry has a link (via a nonvacuum generalization and a static limit) with the Witten bubble spacetime [27] known in five-dimensional, vacuum Kaluza-Klein theory. Finally, with the chosen "redshift function," geodesics and scalar waves turn out to be exactly solvable, thereby leading to tractable as well as interesting consequences.

*sayan@phy.iitkgp.ac.in

To begin, we first state the line element. It is given as

$$ds^2 = -\alpha^2 r^2 dt^2 + \frac{dr^2}{1-\frac{b_0^2}{r^2}} + r^2 d\Omega_2^2, \tag{5}$$

where b_0 and α are two distinct parameters. Asymptotically, the above line element becomes that of a *nonflat, spherical Rindler* type spacetime. Recall that the spherical Rindler spacetime mentioned in [28,29] is globally flat and can be rewritten as Minkowski spacetime via a global coordinate transformation. However, the spacetime obtained in the asymptotic $r \to \infty$ limit of the above-stated line element has a *Rindler* $t - r$ *section* (i.e. $ds^2 = [-\alpha^2 r^2 dt^2 + dr^2] + r^2 d\Omega_2^2$) but is not globally flat. As we will see later, several curvature scalars vanish as $r \to \infty$ and are large but finite near the throat even though the metric is not asymptotically flat. This feature is not uncommon and has been noted in various examples, most notably, say in the so-called Kiselev black holes [30,31] or in the metrics discussed in [32]. Since $r \geq b_0$, there is no singularity anywhere. The spatial section, which is indeed asymptotically flat, has, visibly, the features of the $M = 0$ BE wormhole.

The specific form of g_{00} in the line element in (5) is directly related to the existence of a conformal Killing vector in the geometry. This has been shown and used in [33,34] in the context of wormholes, though the original idea appears in earlier papers [35,36]. Unfortunately, the fact that the line element is not asymptotically flat seems to have been a deterrent in either using it in the wormhole context or analyzing its properties further. Our purpose, in this article, is to fill this gap by studying some of the interesting features of the geometry in (5), which seems to have escaped attention.

One may physically understand the influence of the chosen $g_{00} = -\alpha^2 r^2$ by calculating the frequency shift of a light signal: (i) emitted from the throat and ending up at larger values of r, or (ii) emitted from a larger value of r and reaching the throat at b_0 later. For (ii), one encounters a blue shift whereas in (i) there is a red shift. Thus, an observer at a finite location (infinity) would perceive the presence of a wormhole throat via a finite (an infinite) red shift. This is in contrast to what happens for a black hole where the presence of a horizon is manifest through an infinite red shift (the reason behind the name "red-shift function") of a signal emitted from the horizon, as seen by any observer away from the horizon.

We now move on to further discuss different aspects of this spacetime.

II. THE SPACETIME GEOMETRY AND MATTER

In order to keep things somewhat general let us focus on the following line element:

$$ds^2 = -\alpha^2 r^2 dt^2 + \frac{dr^2}{1-\frac{b(r)}{r}} + r^2 d\Omega_2^2, \tag{6}$$

where $b(r)$ is kept unspecified, as of now. Evaluating the Einstein tensor (we do it in the frame basis) and defining $T_{ij} = \frac{1}{\kappa} G_{ij}$ [from General Relativity (GR)] one can arrive at the NEC inequalities (for a diagonal T_{ij} with $T_{00} = \rho$, $T_{11} = \tau$, $T_{22} = T_{33} = p$, NEC gives $\rho + \tau \geq 0$, $\rho + p \geq 0$):

$$\rho + \tau \geq 0 \Rightarrow \frac{b'r - 3b}{r^3} + \frac{2}{r^2} \geq 0, \tag{7}$$

$$\rho + p \geq 0 \Rightarrow \frac{1}{r^2} \geq 0. \tag{8}$$

The second inequality is trivially true while the first one, as we will see for the specific (BE) choice of $b(r) = \frac{b_0^2}{r}$, yields

$$\rho + \tau \geq 0 \Rightarrow \frac{2r^2 - 4b_0^2}{r^4} \geq 0. \tag{9}$$

Thus the $\rho + \tau \geq 0$ inequality will hold good as long as $r^2 \geq 2b_0^2$, leading to a finite violation in the region $b_0 \leq r < \sqrt{2} b_0$ [33] (see also [37] for discussion on localised NEC violations). It is clear that this localized violation happens only because of the red-shift function we have chosen in this variant of the standard $M = 0$ BE line element (see Fig. 1). The function $\rho + \tau$ has a zero at a location beyond b_0 and this happens because of the choice of g_{00}. In principle, other choices are also possible, for example $g_{00} = -(\alpha r)^m$ with $m \geq 2$ ($m = 2$ being the case considered here).

Let us now turn to evaluating the ANEC given by the integral $\int_{\lambda_1}^{\lambda_2} T_{ij} k^i k^j d\lambda \geq 0$. A quick calculation along radial null geodesics (see [38]) gives the value of the ANEC integral as

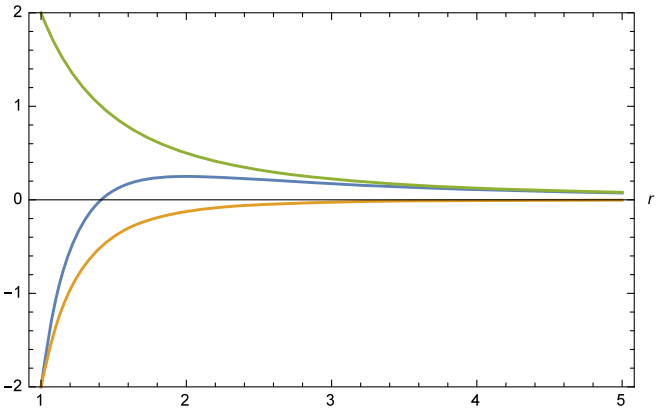

FIG. 1. NEC inequality $\rho + \tau$ (y axis) versus r (x axis) for $M = 0$ BE (yellow), the variant of BE (blue) and the nonflat spherical Rindler type (green). Note that, for BE, violation is for all r, for the variant of BE it happens around the throat and for the nonflat spherical Rindler type there is no violation.

$$\frac{1}{\kappa\alpha}\int_{b_0}^{\infty}\frac{2r^2-4b_0^2}{r^4\sqrt{r^2-b_0^2}}dr=-\frac{2}{3\kappa\alpha b_0^2}. \tag{10}$$

Hence, the ANEC is also violated. However, as is evident from the expression, for a fixed α, the value of the integral becomes smaller and smaller for larger b_0 (i.e. for macroscopically large wormholes). This is expected and not really unusual. If $g_{00}=-1$ (i.e. a standard $M=0$ BE wormhole), then the ANEC integral would have a value equal to $-\frac{\pi}{2\kappa b_0}$. It is indeed clear that one may use both α and b_0 in order to tune the ANEC integral to very small (but negative) values.

As in other scenarios studied earlier [25], we may write the matter required to support the geometry as a sum of two parts—one due to a phantom scalar (violating the NEC) and another satisfying the NEC. More precisely, if we write $\rho=\rho_\phi+\rho_e$, $\tau=\tau_\phi+\tau_e$, and $p=p_\phi+p_e$, then we have

$$\rho=\rho_\phi+\rho_e=\frac{1}{\kappa}\left[\left(-\frac{b_0^2}{r^4}\right)+0\right], \tag{11}$$

$$\tau=\tau_\phi+\tau_e=\frac{1}{\kappa}\left[\left(-\frac{b_0^2}{r^4}\right)+\left(\frac{2r^2-2b_0^2}{r^4}\right)\right], \tag{12}$$

$$p=p_\phi+p_e=\frac{1}{\kappa}\left[\left(\frac{b_0^2}{r^4}\right)+\left(\frac{1}{r^2}\right)\right], \tag{13}$$

where the first terms inside square brackets in the rhs are due to the phantom scalar (which generates the Bronnikov-Ellis geometry) and the rest define the extra piece which is NEC satisfying. This split clearly shows how the redshift function plays a role in confining the NEC violation around the throat only.

The curvature properties of this geometry may be noted through the behavior of the Ricci (R) and Kretschmann (K) scalars given as

$$R=-\frac{4}{r^2};\qquad K=\frac{8}{b_0^2}x^4[x^2(3x^2-2)+1], \tag{14}$$

where $x=\frac{b_0}{r}$ and $0\le x\le 1$. We find that both R and K tend to zero as $r\to\infty$. Moreover, the Ricci scalar R is independent of the value of b_0 and is manifestly negative at all finite r. K, of course, is everywhere positive.

One may be tempted to analyze the NEC and ANEC for a wider class of functions $b(r)$ labeled with a parameter ν and given as

$$b(r)=b_0^\nu r^{1-\nu}. \tag{15}$$

With such a choice, the violation of the local NEC around the throat persists in the region $b_0\le r\le(1+\frac{\nu}{2})^{\frac{1}{\nu}}b_0$. The ANEC integral after evaluation gives

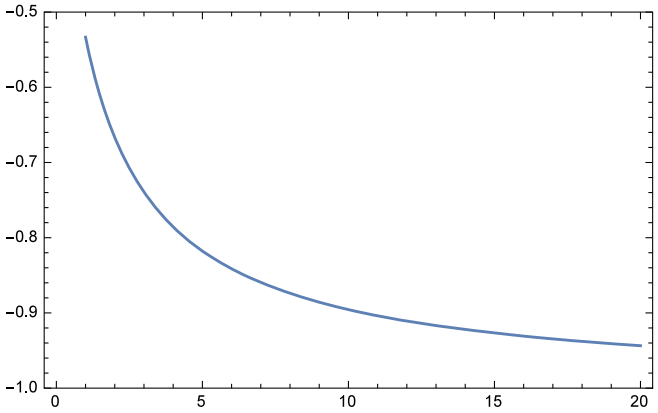

FIG. 2. ANEC integral without the factor $\frac{1}{\kappa\alpha b_0^2}$ (y axis) as a function of the metric parameter ν.

$$\frac{1}{\kappa\alpha}\int_{b_0}^{\infty}\frac{(2r-(\nu+2)b_0^\nu r^{1-\nu})r^{\frac{\nu}{2}}}{r^4\sqrt{r^\nu-b_0^\nu}}dr=-\frac{1}{\kappa\alpha b_0^2}\frac{\sqrt{\pi}\Gamma(\frac{2}{\nu})}{\nu\Gamma(\frac{3}{2}+\frac{2}{\nu})}. \tag{16}$$

We can verify that as ν becomes larger in value the negativity of the integral decreases (see Fig. 2). Also, as observed earlier, for all ν, the violation for fixed α scales as $\frac{1}{b_0^2}$, i.e. for large wormholes the ANEC violation is less.

Thus, in retrospect, we may say that we have variant of the BE line element which represents a Lorentzian wormhole [or a class of wormholes with a one-parameter family of $b(r)$] with a nontrivial red-shift function. Our spacetime requires matter with a local (near the throat) violation of the NEC and an ANEC violation which can be controlled by adjusting the metric parameters (e.g. macroscopically large throat radius).

It is natural to ask—why do we need to bother about such a line element? Is it just to ensure a localized NEC violation? We now elaborate on a precise reason (different from the conformal Killing vector analysis in [33,34]) behind this choice of the red-shift function (i.e. g_{00}), thereby providing our motivations.

III. NONVACUUM WITTEN BUBBLE-LIKE EXTENSIONS

About four decades ago, Witten [27] found a vacuum bubble spacetime in five-dimensional Kaluza-Klein theory by performing a double Wick rotation [27,39] of five-dimensional Schwarzschild geometry ($T=i\chi$ and $\Theta=it+\frac{\pi}{2}$, where T, r, Θ, Φ, ξ are coordinates in the 5D Schwarzschild). The idea there was to demonstrate an instability in the Kaluza-Klein vacuum via this construction. Witten's spacetime is given as

$$ds^2=-r^2dt^2+\frac{dr^2}{1-\frac{b_0^2}{r^2}}+r^2\cosh^2 td\Omega_2^2+\left(1-\frac{b_0^2}{r^2}\right)d\chi^2, \tag{17}$$

where $\chi = R\xi$ and $0 \leq \xi \leq 2\pi$ (periodic), R a constant. Also $b_0 \leq r < \infty$. The spacetime topology is $R^2 \times S^2 \times S^1$. Geodesics [40] and scalar waves [41] in the Witten bubble have been studied in some detail in the past.

One can generalize this spacetime to a nonvacuum scenario by introducing new parameters. Such a variant could be given by a line element,

$$ds^2 = -\alpha^2 r^2 dt^2 + \frac{dr^2}{1-\frac{b_0^2}{r^2}} + r^2 \cosh^2 \rho_1 t d\Omega_2^2 + \left(1-\frac{b_0^2}{r^2}\right) d\chi^2, \tag{18}$$

where $\rho_1 \neq \alpha > 0$.

The purpose behind our construction is to eventually take a limit $\rho_1 = 0$, which will reduce the spacetime in (18) to a static one. Such a static spacetime will have its $\chi =$ constant section as the four-dimensional geometry we have proposed in the earlier sections of this article. Note that the Witten bubblelike spacetime in (18) cannot be obtained as a double Wick rotation of 5D Schwarzschild, more so because it is nonvacuum.

It will be useful to write down the Einstein tensor for this generalized spacetime in (18) and note its non–vacuum character as well as the nature of the required matter *vis-á-vis* the energy conditions (NEC). We find (in the frame basis and using five-dimensional GR),

$$T_{00} = \frac{1}{\kappa_5} G_{00} = \rho = \frac{1}{\kappa_5 r^2}\left(\frac{\rho_1^2}{\alpha^2} - 1\right) \tanh^2 \rho_1 t, \tag{19}$$

$$T_{11} = \frac{1}{\kappa_5} G_{11} = \tau = -\frac{1}{\kappa_5 r^2}\left(\frac{\rho_1^2}{\alpha^2} - 1\right)(2 + \tanh^2 \rho_1 t), \tag{20}$$

$$T_{22} = T_{33} = p = \frac{1}{\kappa_5} G_{22} = -\frac{1}{\kappa_5 r^2}\left(\frac{\rho_1^2}{\alpha^2} - 1\right), \tag{21}$$

$$T_{44} = p_e = \frac{1}{\kappa_5} G_{55} = -\frac{1}{\kappa_5 r^2}\left(\frac{\rho_1^2}{\alpha^2} - 1\right)(2 + \tanh^2 \rho_1 t), \tag{22}$$

where κ_5 is the five-dimensional generalization of κ.

It is easy to verify that the NEC ($\rho + \tau \geq 0$, $\rho + p \geq 0$, $\rho + p_e \geq 0$) holds good as long as $\rho_1 \leq \alpha$. For $\rho_1 = \alpha$ we get back the vacuum Witten bubble spacetime. On the other hand, the generalized spacetime has a viable $\rho_1 = 0$ limit (since ρ_1 and α are independent parameters). In this limit, we have a static spacetime given as

$$ds^2 = -\alpha^2 r^2 dt^2 + \frac{dr^2}{1-\frac{b_0^2}{r^2}} + r^2 d\Omega_2^2 + \left(1-\frac{b_0^2}{r^2}\right) d\chi^2 \tag{23}$$

for which the matter required has the following peculiar character:

$$\rho = 0, \qquad \tau = \frac{1}{\kappa_5}\frac{2}{r^2}, \tag{24}$$

$$p = \frac{1}{\kappa_5}\frac{1}{r^2}, \qquad p_e = \frac{1}{\kappa_5}\frac{2}{r^2}. \tag{25}$$

Interestingly, this stress energy also satisfies the NEC. Notice the complete absence of b_0 in the expressions in (19)–(22) and also in (24)–(25). This happens only when we choose $b(r) = \frac{b_0^2}{r}$, not for all $b(r)$, as we can easily see from the following discussion.

Let us try to understand how the NEC holds by considering a somewhat general five-dimensional spacetime given as

$$ds^2 = -\alpha^2 r^2 dt^2 + \frac{dr^2}{1-\frac{b(r)}{r}} + r^2 d\Omega_2^2 + \left(1-\frac{b(r)}{r}\right) d\chi^2, \tag{26}$$

where $b(r)$ is an unspecified function to start with. If we write down the NEC inequalities $\rho + \tau \geq 0$, $\rho + p \geq 0$ (these are the only two which are relevant since $\tau = p_e$), then we can check that we obtain

$$\rho + \tau \geq 0 \Rightarrow \frac{b'' r^2 - b' r - 3b}{2r^3} + \frac{2}{r^2} \geq 0, \tag{27}$$

$$\rho + p \geq 0 \Rightarrow \frac{1}{r^2} \geq 0. \tag{28}$$

In the usual four dimensional wormhole spacetime (say, the one considered earlier), the first of the above inequalities [Eq. (27), i.e. the $\rho + \tau \geq 0$ inequality] results in the requirement $b' r - b \geq 0$, near the wormhole throat. This contradicts the requirement on a wormhole shape as found from embedding features, namely, $b - b' r > 0$ [3]. In the five-dimensional geometry considered here, the $\rho + \tau \geq 0$, does not quite contradict the embedding criterion for a wormhole shape, as mentioned above. For example, if we choose a class of functions given as $b(r) = b_0^\nu r^{1-\nu}$ we find the inequality in (27) to be

$$\frac{1}{2r^2}\left(\frac{b_0}{r}\right)^\nu (\nu^2 - 4) + \frac{2}{r^2} \geq 0, \tag{29}$$

which always holds for all $\nu \geq 2$. In principle, there could be many functions $b(r)$ for which the NEC will be satisfied.

The above five-dimensional static spacetime can indeed serve as an example of a five-dimensional wormhole satisfying the NEC (in fact, all energy conditions). Earlier work [28] addressed the wormhole features of the original nonstatic Witten-bubble spacetime. Here, we have introduced a parameter ρ_1, using which we can obtain a static five-dimensional wormhole. The nature of the

matter could be questioned—the energy density is identically zero, as seen from the frame of a static observer! Despite this peculiarity, the spacetime probably provides us with a counterexample (albeit via extra dimensions and perhaps, entirely mathematical) where energy condition violating matter does not seem to be a precondition for the existence of a wormhole in GR with extra dimensions. Note that near the throat the extra dimension vanishes, whereas in the asymptotic regions it exists with a constant radius. A constant χ (constant extra dimensional) section of the five-dimensional static geometry is the spacetime we have been talking about in our previous sections. The meaning and relevance of the higher dimensional spacetimes mentioned in this section may surely be explored further in future.

IV. GEODESIC MOTION

Let us now return to the original four-dimensional spacetime which appears as a $\chi =$ constant section of the static, five-dimensional spacetime mentioned above. We now try to find the timelike and null geodesics in this four-dimensional spacetime.

The null and timelike geodesics satisfy the condition

$$-\alpha^2 r^2 \dot{t}^2 + \frac{\dot{r}^2}{1-\frac{b_0^2}{r^2}} + r^2\dot{\theta}^2 + r^2\sin^2\theta\dot{\phi}^2 = -\gamma, \quad (30)$$

where $\gamma = 1$ for timelike and $\gamma = 0$ for null. The overdot here denotes a derivative with respect to the parameter τ labeling points on the geodesics.

We may work with the choice $\theta = \frac{\pi}{2}$ since it satisfies the θ geodesic equation. We also have two constants of motion E and L given as

$$\dot{t} = \frac{E}{\alpha^2 r^2}, \qquad \dot{\phi} = \frac{L}{r^2}. \quad (31)$$

Using the above in the timelike geodesic condition ($\gamma = 1$) we arrive at the following equations:

$$\frac{dr}{dt} = \pm\frac{\alpha^2}{E}\sqrt{(d_0^2 - r^2)(r^2 - b_0^2)}, \quad (32)$$

$$\frac{d\phi}{dt} = \frac{L}{E}\alpha^2, \quad (33)$$

where $d_0^2 = \frac{E^2}{\alpha^2} - L^2 > 0$.

One may interpret the expression for $\frac{dr}{dt}$ using an effective potential. This leads to the definition of $V(r)$:

$$\left(\frac{dr}{dt}\right)^2 = -\frac{\alpha^4}{E^2}(r^2 - d_0^2)(r^2 - b_0^2) = -V(r). \quad (34)$$

Figure 3 (figure on the left) shows the graph of $V(r)$ where the $V = 0$ horizontal line intersects $V(r)$ at b_0 and d_0 (end points of the periodic motion, see below). $V(r)$ here is a well potential whereas in $M = 0$ BE geometry the corresponding $V(r)$ has a barrier near the throat–the difference exclusively driven via the chosen red-shift function.

We first note that circular orbits are possible for $r = d_0$ and also at $r = b_0$ (with a constraint $b_0^2\alpha^2 = E^2 - \alpha^2 L^2$).

General periodic solutions to the r equation exist for both $L = 0$ and $L \neq 0$. The solution ($L \neq 0$) is given as

$$r(t) = b_0 nd\left[d_0\frac{\alpha^2}{E}t; \frac{d_0^2 - b_0^2}{d_0^2}\right], \quad (35)$$

$$\phi(t) = \frac{L\alpha^2}{E}t, \quad (36)$$

where "$nd[x, k]$" is a periodic Jacobian elliptic function with real periodicity given by $2K(k)$ [$K(k)$ denotes the elliptic integral of the third kind]. Figure 3 (figure on the right side) shows a graph for $r(t)$. It is possible to integrate the relation $\dot{t} = \frac{E}{\alpha^2 r^2}$ and obtain an expression of $\tau(t)$. We have checked (not presented here) that $\tau(t)$ is monotonically increasing and given in terms of various Jacobi elliptic functions. Note further that in the limit $d_0 \to b_0$ (i.e. $k \to 0$) one gets back the circular orbit $r = b_0$ because $nd[x, 0] = 1$.

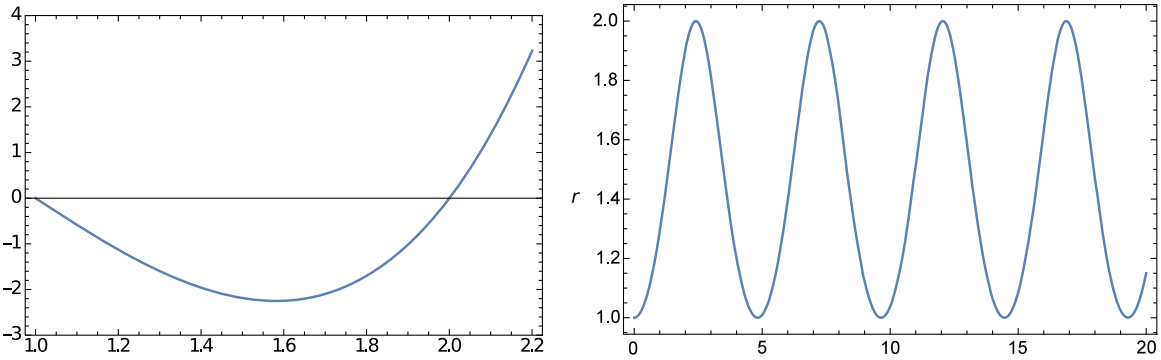

FIG. 3. Left: effective potential $V(r) \times E^2$. Right: $r(t)$ as in Eq. (35). Values for both figures: $\alpha = 1$, $L = 1$, $E = \sqrt{5}$, $b_0 = 1$, $d_0 = 2$. The right figure represents the Jacobian elliptic function "nd."

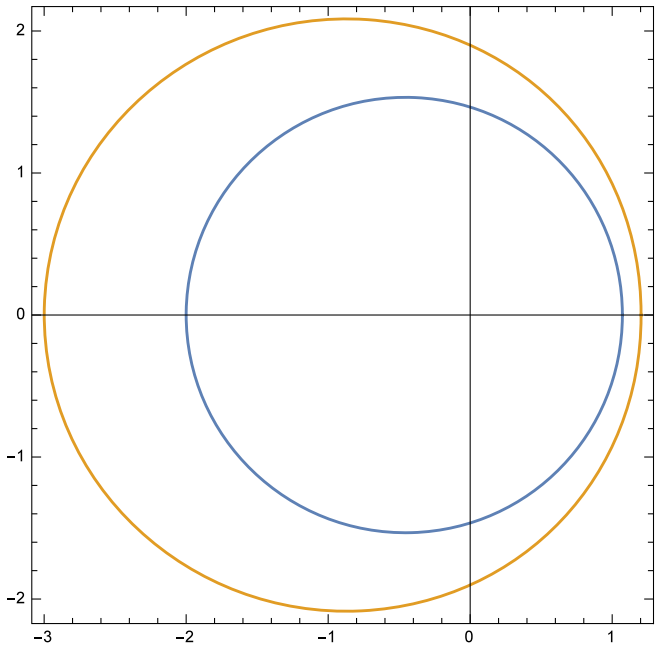

FIG. 4. Polar plot of closed orbits with (i) $d_0 = 2$, $b_0 = 1.07183$, $L = 3$, $E = \sqrt{13}$, $\alpha = 1$, $k = 0.712795$ [blue], (ii) $d_0 = 3$, $b_0 = 1.20342$, $L = 4$, $E = 5$, $\alpha = 1$ [yellow].

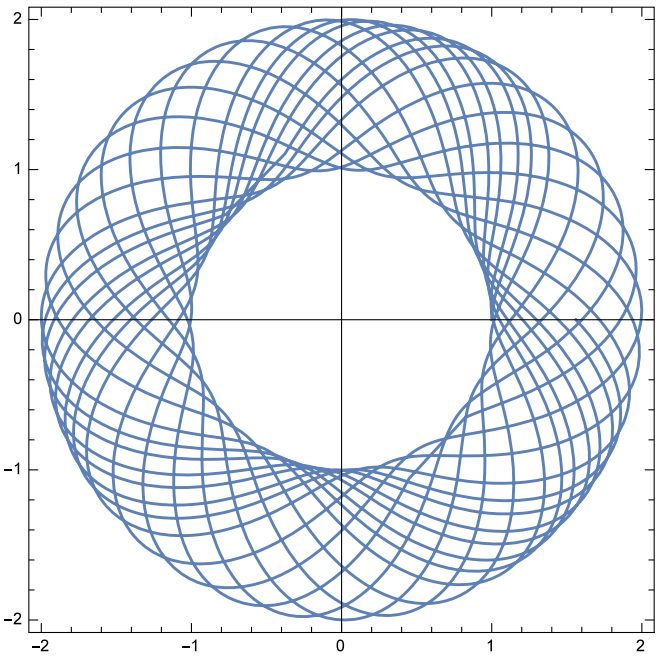

FIG. 5. Polar plot of open, bounded periodic orbit for $k = 0.75$, $L = 1$, $E = \sqrt{5}$, $d_0 = 2$, $b_0 = 1$, $\alpha = 1$.

We may also write the solution as

$$r(\phi) = b_0 nd\left[d_0\frac{\phi}{L};\frac{d_0^2 - b_0^2}{d_0^2}\right]. \tag{37}$$

For closed orbits, we require

$$\frac{2\pi d_0}{L} = 2K(k), \tag{38}$$

where $k = \frac{d_0^2 - b_0^2}{d_0^2} < 1$.

In time $t_c = \frac{2K(k)E}{d_0\alpha^2}$ the particle returns to $r = b_0$ after a full circuit in ϕ. To illustrate this feature on closed and open (attractor) orbits we give the following example. Take $d_0 = 2$, $\alpha = 1$, $E = \sqrt{13}$, and $L = 3$. The condition for closed orbits turns out to be $K(k) = \frac{2\pi}{3}$. Solving, we get $k = 0.712795$. Hence, $b_0 = 1.07183$. Using these numerical values one can obtain the blue curve in Fig. 4 which represents a closed orbit with minimum and maximum r given as $r = 1.07183$ and $r = 2$. The yellow curve in Fig. 4 is for a different set of parameters. In contrast, if we do not use the condition $K(k) = \pi\frac{d_0}{L}$ in order to find k, we end up with an open orbit for which the values of r are confined between b_0 and d_0 (see Fig. 5 where $d_0 = 2$, $b_0 = 1$, $k = 0.75$, $L = 1$, $\alpha = 1$, and $E = \sqrt{5}$, as in Fig 3.). Thus, both closed and open periodic orbits exist under specific conditions.

When $L = 0$, it is clear that ϕ is a constant. We also have $d_0 = \frac{E}{\alpha}$. Thus, we end up with

$$r(t) = b_0 nd\left[\alpha t;\frac{E^2 - b_0^2\alpha^2}{E^2}\right]. \tag{39}$$

The trajectory now is at a fixed ϕ and the particle oscillates up and down from b_0 to d_0 and vice versa. It is easy to see that the particle starting from $r = b_0$ at $t = 0$ will return to $r = b_0$ in time $\alpha t_c = 2K(k)$.

Thus, for both $L = 0$ and $L \neq 0$ one has periodic motion and we are able to find the functional dependence exactly. The closed orbits as well as the open bounded orbits found here are unique to this generalized BE spacetime and is absent in the standard (i.e. $f = 0$) BE spacetime usually studied. Furthermore, it is useful to note that the static geometry representing the generalization of the Witten bubble will have the same geodesics for $\chi =$ constant (which solves the χ geodesic equation).

Another important and interesting quantity which can be easily calculated is the expansion Θ of a timelike geodesic congruence generated by the geodesic vector field u^i given as

$$u^i \equiv \left(\frac{E}{\alpha^2 r^2}, \frac{1}{r^2}\sqrt{(r^2 - b_0^2)(d_0^2 - r^2)}, 0, \frac{L}{r^2}\right). \tag{40}$$

A straightforward calculation leads to the expression for Θ as

$$\Theta = \nabla_i u^i = \frac{2b_0^2(r^2 - d_0^2) - d_0^2(r^2 - b_0^2) + 3(r^2 - b_0^2)(d_0^2 - r^2)}{r^3\sqrt{(r^2 - b_0^2)(d_0^2 - r^2)}}. \tag{41}$$

It is easy to see that in the $r \to b_0$ and $r \to d_0$ limits the expansion Θ diverges to negative infinity, indicating benign focusing. In particular, a timelike geodesic congruence which starts out at some point between b_0 and d_0 with an initially negative expansion will eventually focus at b_0 or d_0—a result which follows from the well-known focusing theorem obtained as a conclusion from the Raychaudhuri equation.

It is even more easy to find the null geodesics though it is not periodic motion. One can easily check that the radial null geodesics ($L = 0$, ϕ constant) in this spacetime are given as

$$r = b_0 \cosh \alpha t. \tag{42}$$

The trajectory represents a photon starting out at the throat and escaping to infinity, along a curve with ϕ fixed.

When $L \neq 0$, i.e. for the nonradial null geodesics, the solution turns out to be

$$r(t) = b_0 \cosh \frac{d_0 \alpha^2}{E} t, \qquad \phi = \frac{\alpha^2 L}{E} t. \tag{43}$$

Here, the photon spirals away to infinity because of the time variation of ϕ.

It is worth noting that the null geodesics found in this geometry are also different from those of the BE geometry. For example, for $L = 0$, in BE spacetime, one gets

$$r(t) = r(\tau) = \sqrt{b_0^2 + t^2} = \sqrt{b_0^2 + E^2 \tau^2}, \tag{44}$$

which is functionally different from the expression in (42) above.

The periodic and nonperiodic behavior of timelike and null geodesics, respectively, is somewhat reminiscent of geodesics in anti–de Sitter spacetime where the radial null geodesics exhibit a runaway to infinity at finite t, whereas, the timelike geodesics have periodic behavior. A sort of reason behind this "similar" behavior could be attributed to the fact that $g_{00} = -\alpha^2 r^2$ for our spacetime and for anti–de Sitter spacetime, it is simply $g_{00} = -(1 + \alpha^2 r^2)$.

Thus, one may say that all geodesics in the proposed spacetime wormhole are known exactly, which we feel is a satisfying feature for this geometry. We also obtain a fairly wide variety of trajectories—periodic, nonperiodic, open, bounded and closed. If at all, such geometries are ever deemed to be observationally relevant, then the diverse behavior of test particles, as described above, could yield useful signatures.

We now turn to the final topic of discussion—scalar wave propagation—which, as we will show, is also exactly solvable!

V. SCALAR WAVES

The propagation of massless scalar waves in this spacetime geometry is governed by the equation:

$$\Box \phi = 0. \tag{45}$$

Studying such scalar waves amounts to an analysis of scalar perturbations. One can consider the perturbations as those for the scalar which generates part of the matter required to support the geometry (see earlier discussion in Sec. II).

Assuming $\phi = T(t)R(r)Y(\theta, \phi)$, one can easily separate variables and look for solutions with $T(t) = e^{\pm i\omega t}$. The angular part $Y(\theta, \phi)$ is given in terms of the spherical harmonics $Y_{mn}(\theta, \phi)$. Using new coordinates $r = b_0 \cosh \xi$, one arrives at the equation for $R(\xi)$ as

$$\frac{d^2R}{d\xi^2} + 2 \tanh \xi \frac{dR}{d\xi} + \left(m(m+1) + \frac{\omega^2}{\alpha^2} \right) \quad R = 0. \tag{46}$$

A further substitution $R = \mathrm{sech}\xi A(\xi)$ results in a surprisingly simple equation for A:

$$\frac{d^2A}{d\xi^2} + \left(\frac{\omega^2}{\alpha^2} + m(m+1) - 1 \right) A = 0. \tag{47}$$

The final solution for $R(r)$ is therefore given as

$$R(r) = \frac{b_0}{r} \left(C_1 \sin \left[p \cosh^{-1} \frac{r}{b_0} \right] + C_2 \cos \left[p \cosh^{-1} \frac{r}{b_0} \right] \right), \tag{48}$$

where

$$p = \sqrt{\frac{\omega^2 - \alpha^2}{\alpha^2} + m(m+1)} \tag{49}$$

and C_1, C_2 are integration constants. Note that for $m = 0$, p is real (imaginary) for $\omega > \alpha$ ($\omega < \alpha$). For all other $m \neq 0$, p is real. The solution represents spherical waves with decreasing amplitude as one moves away from the throat towards infinity (see Fig. 6). Thus, the spacetime is stable against such scalar perturbations—a fact which adds to its viability as a geometry worth considering. Surely, more general perturbations (e.g. axial and polar gravitational ones) have to be explored in order to understand the stability issue in a more complete way.

We may also contrast the behavior of scalar wave propagation in this geometry with corresponding scenarios in the asymptotic nonflat, spherical Rindler type spacetime and in the $M = 0$ BE spacetime. In the nonflat spherical Rindler case, the radial part $R(r)$ of ϕ is generically given by power laws of the type r^{-s} ($s > 0$)—thus the decay is not oscillatory. In the Bronnikov-Ellis spacetime, the solution of the equation for $R(r)$ is given by the rather

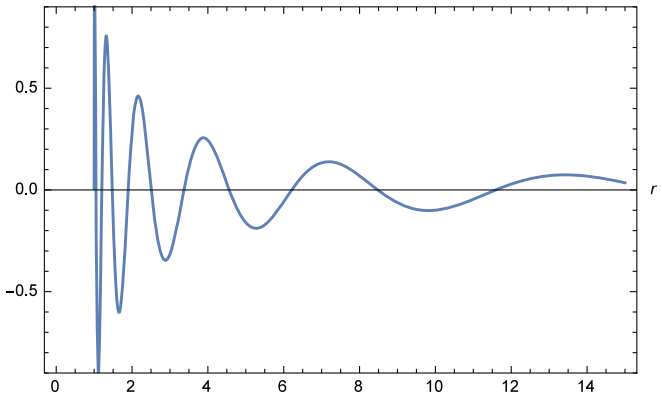

FIG. 6. The radial wave function $R(r)$, assuming $\alpha = 1$, $b_0 = 1$, $\omega^2 = 99$, $C_2 = 0$, $C_1 = 1$.

complicated radial oblate spheroidal functions, as noted and discussed many years ago in [4].

VI. CONCLUDING REMARKS

Among many possibilities that emerge from this work, one which could be quite important concerns the geometry arising as the static limit of the generalized Witten bubble-like spacetime in 5D, which can be supported with matter satisfying the NEC. This spacetime has wormhole features and its constant extra dimension section is the 4D geometry discussed here. We have shown that the presence of the extra dimension as well as the choice of the red-shift function, somehow manages to evade the NEC violation in this higher dimensional spacetime. It is clear that this feature will persist with more extra dimensions. In addition, a further generalization of Eq. (23) with the higher dimensional line element rewritten as

$$ds^2 = -e^{2\psi(r)}dt^2 + \frac{dr^2}{1-\frac{b(r)}{r}} + r^2 d\Omega_2^2 + \left(1-\frac{d(r)}{r}\right)d\chi^2, \tag{50}$$

where $b(r) \neq d(r)$ and $\psi(r)$ an additional function, also seems to suggest viable wormhole spacetimes [for chosen $b(r)$, $d(r)$, and $\psi(r)$] in vacuum or with any required matter satisfying/violating the NEC [42]. Thus, our work indicates a fairly broad class of examples of NEC satisfying wormholes within the framework of higher dimensional GR. Strangely, if one considers the four-dimensional section (constant χ) as an independent geometry (as we have done in this paper) in four-dimensional GR, one ends up with localized NEC violation around the wormhole throat. Further future studies may help us in understanding the above-mentioned intriguing features.

It also turns out that geodesic motion as well as scalar wave propagation can be solved exactly for this spacetime, in terms of known functions. This feature does not really exist in too many spacetimes which arise in GR or other theories of gravity. In addition, the closed orbits and attractors noted in timelike geodesic motion provides useful signatures which may help in characterizing the geometry.

Finally, a science fiction enthusiast may wonder if our 4D spacetime wormhole is traversable. We have found that (not shown here) choosing the dimensionless number αb_0 appropriately we can indeed have a traversable (for humans) wormhole. The tidal force constraints will, as always, restrict the possible allowed value of the throat radius. However, it is necessary to understand the sense of traversability here, with special reference to the fact that timelike geodesics are all bounded between $r = b_0$ and $r = d_0$, though the value of d_0 can be large via choices of E, α and L. Alternatively, one may consider [33] taking a timelike piece of this geometry, say, between $r = b_0$ and some $r = r_0 > b_0$ and join the boundary at r_0 with vacuum Schwarzschild. In such a case, one obtains an asymptotically flat traversable wormhole via cut and paste with a thin shell at r_0 having matter violating the energy conditions.

It goes without saying that our work is largely theoretical (bordering on the exotic, to say the least!) and has no link with observations (as of now). However, we do feel that our results provide an interesting outing, illustrating the links between wormholes, energy conditions, extra dimensions on one hand and exactly solvable geodesics and scalar wave propagation on the other, with curious consequences which may perhaps motivate future research. The role of the specially chosen "red-shift function" ($g_{00} = -\alpha^2 r^2$) and the link with the Witten bubble are both crucial and novel elements which have guided our pursuits in this article.

[1] K. A. Bronnikov, Acta Phys. Pol. B **4**, 251 (1973).
[2] H. Ellis, J. Math. Phys. (N.Y.) **14**, 104 (1973).
[3] M. S. Morris and K. S. Thorne, Am. J. Phys. **56**, 395 (1988).
[4] S. Kar, D. Sahdev, and B. Bhawal, Phys. Rev. D **49**, 853 (1994).
[5] A. Das and S. Kar, Classical Quantum Gravity **22**, 3045 (2005).
[6] D. I. Novikov, A. G. Doroshkevich, I. D. Novikov, and A. A. Shatskiy, Astronomy Reports **53**, 1079 (2009).
[7] H. Huang and J. Yang, Phys. Rev. D **100**, 124063 (2019).
[8] P. Canate, J. Sultana, and D. Kazanas, Phys. Rev. D **100**, 064007 (2019).
[9] N. Tsukamoto and Y. Gong, Phys. Rev. D **97**. 084051 (2018).

[10] X. Y. Chew, B. Kleihaus, and J. Kunz, Phys. Rev. D **94**, 104031 (2016).
[11] N. Tsukamoto, Phys. Rev. D **94**, 124001 (2016).
[12] K. K. Nandi, A. A. Potapov, R. Izmailov, A. Tamang, and J. C. Evans, Phys. Rev. D **93**, 104044 (2016).
[13] M. Zhou, A. Cardenas-Avendano, C. Bambi, B. Kleihaus, and J. Kunz, Phys. Rev. D **94**, 024036 (2016).
[14] B. Kleihaus and J. Kunz, Phys. Rev. D **90**, 121503(R) (2014).
[15] R. Takahashi and H. Asada, Astrophys. J. Lett. **768**, L16 (2013).
[16] C-M. Yoo, T. Harada, and N. Tsukamoto, Phys. Rev. D **87**, 084045 (2013).
[17] K. Nakajima and H. Asada, Phys. Rev. D **85**, 107501 (2012).
[18] Y. Toki, T. Kitamura, H. Asada, and F. Abe, Astrophys. J. **740**, 121 (2011).
[19] F. Abe, Astrophys. J. **725**, 787 (2010).
[20] T. Damour and S. N. Solodukhin, Phys. Rev. D **76**, 024016 (2007).
[21] J. P. S. Lemos and O. B. Zaslavskii, Phys. Rev. D **78**, 024040 (2008).
[22] R. A. Konoplya, Phys. Lett. B **784**, 43 (2018).
[23] R. A. Konoplya and A. Zhidenko, J. Cosmol. Astropart. Phys. 12 (2016) 043.
[24] S. Aneesh, S. Bose, and S. Kar, Phys. Rev. D **97**, 124004 (2018).
[25] P. Dutta Roy, S. Aneesh, and S. Kar, Eur. Phys. J. C **80**, 850 (2020).
[26] K. A. Bronnikov, R. A. Konoplya, and T. Pappas, Phys. Rev. D **103**, 124062 (2021).
[27] E. Witten, Nucl. Phys. **B195**, 481 (1982).
[28] H. Culetu, J. Korean Phys. Soc. **57**, 419 (2010).
[29] V. Balasubramanian, B. D. Chowdhury, B. Czech, and J. de Boer, J. High Energy Phys. 10 (2013) 220.
[30] V. V. Kiselev, Classical Quantum Gravity **20**, 1187 (2003).
[31] M. Visser, Classical Quantum Gravity **37**, 045001 (2020).
[32] G. Clement and C. Leygnac, Phys. Rev. D **70**, 084018 (2004).
[33] C. G. Boehmer, T. Harko, and F. S. N. Lobo, Phys. Rev. D **76**, 084014 (2007).
[34] P. K. F. Kuhfittig, Eur. Phys. J. C **75**, 357 (2015).
[35] L. Herrera, J. Jimenez, L. Leal, J. Ponce de Leon, M. Es-culpi, and V. Galina, J. Math. Phys. (N.Y.) **25**, 3274 (1984); L. Herrera and J. Ponce de Leon, J. Math. Phys. (N.Y.) **26**, 2302 (1985).
[36] R. Maartens and M. S. Maharaj, J. Math. Phys. (N.Y.) **31**, 151 (1990).
[37] M. Azreg-Aïnou, J. Cosmol. Astropart. Phys. 07 (2015) 037.
[38] M. Visser, *Lorentzian Wormholes: From Einstein to Hawking* (AIP Press, Woodbury, New York, 1997).
[39] A. Bachelot, Commun. Math. Phys. **351**, 599 (2017).
[40] D. Brill and M. D. Matlin, Phys. Rev. D **39**, 3151 (1989).
[41] B. Bhawal and C. V. Vishveshwara, Phys. Rev. D **42**, 1996 (1990).
[42] S. Kar (to be published).

Correction: The second sentence in the penultimate paragraph in the Introduction contained an error and has been replaced.